Characteristics of piezoelectric polymer film sensors with solution-processable graphene-based electrode materials

Satu Rajala, Sampo Tuukkanen and Jouko Halttunen

***Abstract*—The sensor characteristics of piezoelectric polyvinylidenefluoride (PVDF) sensors with solution-processable electrode materials were studied. The electrodes were solution-processed on 28 µm thick PVDF film. Two graphene-based printable inks, ink-jet and screen formulated ink, were used. Sensors with evaporated metal electrodes were used as a reference to compare the properties of novel sensor structures. The sensor characteristics studied here were sensitivity, nonlinearity, hysteresis and the effects of frequency and temperature. The sensor sensitivity measurements revealed mean sensitivities of (31.1 ± 1.4) pC/N for the reference sensors and (26.2 ± 2.2) pC/N and (21.4 ± 1.3) pC/N for the sensors with graphene-based ink-jet and screen formulated ink electrodes, respectively. The sensor characteristics of the novel sensors were found to be similar to those of the reference sensors. The new sensors are linear, hysteresis error is negligible, and the operation under changing frequency (up to 100 Hz) is rather stable. Change in ambient temperature somewhat affects the sensor sensitivities. The sensors presented here can be used in several sensing applications, e.g. in plantar pressure distribution measurements.**

***Index Terms*—Electrodes, piezoelectric films, piezoelectric transducers.**

I. Introduction

Recently, there has been increasing interest in printed and solution-processed sensors. The use of printing and solution-processing technologies is an additive process that has advantages when compared to conventional subtractive lithography-based processing methods. For example, the manufacturing process is simplified due to the decreased number of process steps. Also the amount of waste is decreased, since only the required amount of material is placed in the desired location.

Carbon based nanomaterials, such as graphene [1], [2], [3], are promising materials for future electronics, photonics and material sciences. For instance, these materials can produce stretchable [4] and transparent [5] electrodes for sensor applications. At present, carbon based nanomaterials can be solution-processed which enables the use of printing techniques providing a way to low-cost and high throughput mass production of electronic devices [6]. The carbon based materials are also considered as environmental friendly materials, thus making the products potentially disposable in the end of their life-cycle.

Polyvinylidenefluoride (PVDF) is a piezoelectric plastic material that generates a charge when it is mechanically deformed [7]. Several applications for thin and flexible pressure sensors can be found, e.g. measurement of plantar pressure distribution [8]. The measurement of plantar pressure distribution is established as an important technique for identifying feet that are at risk of ulceration [9]. The focus here is to study the sensor characteristics of discrete pressure sensors based on PVDF sensor material with solution-processable electrode materials. Solution-processable electrode materials are used to overcome the problem concerning the temperature sensitivity of the PVDF sensor material [10] and also, to enable mass manufacturing of the discrete and matrix PVDF sensors in a desired and customized shape and size.

Several attempts to manufacture electrodes on PVDF material have been made. Recently, various solution-processable electrode materials, e.g. carbon nanotube-cellulose composite, poly(3,4-ethylenedioxythiophene):poly(styrene sulfonate) (PEDOT:PSS), carbon ink and silver flake ink, have been tested as electrode materials by Tuukkanen *et al.* [10], [11]. Metal electrode fabrication on PVDF material using ink-jet printing has also been previously demonstrated by Kärki *et al.* [12]. The required high-temperature sintering step (150 °C) needed in metal electrode fabrication, however, causes limitations in sensor functionality [12]. Seminara *et al.* used inkjet printing to deposit patterned metal layers on PVDF material to realize scalable, bendable and low-cost sensing system for large area artificial skin [13]. Lee *et al.* fabricated flexible organic film speakers with ion-assisted-reaction (IAR) treated PVDF as the active layer and PEDOT:PSS materials

Manuscript received May 15, 2014.

S. Rajala is with the Department of Automation Science and Engineering, Tampere University of Technology, P.O. Box 692, Tampere, FI-33101 Finland (e-mail: satu.rajala@tut.fi).

S. Tuukkanen is with the Department of Electronics and Communications Engineering, Tampere University of Technology, P.O. Box 692, Tampere, FI-33101 Finland (e-mail sampo.tuukkanen@tut.fi). Present address: Department of Material Science, School of Chemical Technologies, Aalto University, Espoo, Finland.

J. Halttunen is with the Department of Automation Science and Engineering, Tampere University of Technology, P.O. Box 692, Tampere, FI-33101 Finland (e-mail: jouko.halttunen@tut.fi).

with various organic solvents, indium tin oxide (ITO) or copper (Cu) as the electrodes [14]. Schmidt *et al*. developed both airbrush and inkjet printing methods for applying PEDOT:PSS electrodes to PVDF sheets [15]. Zirkl *et al*. demonstrated an all-printed matrix sensor array using P(VDF-TrFE) as the sensor ink [16]. Also Rendl *et al*. have used printable piezoelectric PVDF-TrFE film as an active layer in their sensors and conductive polymer (PEDOT:PSS) and carbon as electrode materials [17]. Despite these promising results obtained with PVDF sensors with printed or solution-processed electrodes, the systematic testing of sensor characteristics studied here is not done before. The systematic evaluation of sensor characteristics provides information on the sensor behavior under changing conditions and is thus needed before the sensors can be successfully used in different sensing applications.

Here the electrodes are solution-processed on a 28 µm thick unmetallized PVDF material. Two commercially available graphene-based ink-jet and screen formulated printable inks are used as solution-processable electrode materials. These electrode materials are compatible with flexible substrates, and especially, they can be used with temperature sensitive PVDF films since they do not require subsequent heating treatments as do most metal particle-based printable inks. Further, the ink-jet formulated graphene-based ink provides transparency of the PVDF sensors. Fabrication of the graphene-based electrodes on the PVDF substrate is a simple one-step process followed by a short low temperature heat treatment to evaporate the solvent from the ink. The solution-processed electrodes are characterized by using sheet resistance measurements and adhesion tests. Sensors with evaporated metal electrodes (copper) are used as a reference to compare the properties of the novel sensor structures. The sensor operation characteristics to be studied here are sensitivity, nonlinearity, hysteresis and the effects of frequency and temperature. Here the sensor characteristics are evaluated only in operation under the force normal to the sensor surface.

The structure of this paper is as follows. Section II describes the materials and methods used in the study. Section III introduces the obtained results and in Section IV the results are discussed.

II. MATERIALS AND METHODS

A. Piezoelectric polymer PVDF

PVDF ($(CH2 – CF2)_n$) is a piezoelectric material having a solid structure with approximately 50-65 % crystallinity [18]. The morphology consists of crystallites dispersed within amorphous regions [19]. The manufacturing process of PVDF material is described e.g. in references [18] and [7]. Briefly, the PVDF sheet is stretched at the temperature close to the melting point (around 175 °C) to cause a chain packing of the molecules into piezoelectric β crystalline phase. These dipole moments are randomly oriented and result in zero net polarization. In the polarization stage the stretched polymer is exposed to a high electric field to generate piezoelectric properties. The molecular dipoles are oriented in the direction of the field and a net polarization is formed when the material cools down. Finally, the film is metallized to provide electrodes.

TABLE I
TYPICAL PROPERTIES OF 28 µM THICK PVDF MATERIAL [7].

Property	Symbol	PVDF 28 µm	Unit
Piezoelectric coefficient	d_{33}	$-33\cdot10^{-12}$	CN^{-1}
	d_{31}	$23\cdot10^{-12}$	
Young's modulus	Y	$2\cdot10^{9}$-$4\cdot10^{9}$	Nm^{-2}
Pyroelectric coefficient	p	$30\cdot10^{-6}$	$Cm^{-2}K^{-1}$
Capacitance	C	380	$pFcm^{-2}$
Permittivity	ε	$106\cdot10^{-12}$-$113\cdot10^{-12}$	Fm^{-1}
Relative permittivity	$\varepsilon/\varepsilon_0$	12-13	-
Mass density	ρ	$1.78\cdot10^{3}$	kgm^{-3}
Dynamic pressure range	p	$1\cdot10^{-6}$-$5\cdot10^{9}$	Pa
Temperature range	T	-40 to 80…100	°C

The change in film thickness due to an external force compressing the film generates a charge and thus, a voltage to appear at the electrodes. The piezoelectric coefficient d_{mn} is related to the electric field produced by a mechanical stress; the first suffix m = 1, 2, 3 refers to the electrical axis and the second n = 1, 2, …, 6 to the mechanical axis [7]. The d_{mn} is a third-rank tensor conventionally expressed in terms of 3 x 6 matrix, however, crystal symmetry reduces the number of independent piezoelectric coefficients [20]. The symmetry class of the poled polymer is orthorhombic 2 mm [21] for which the matrix can be written as [22]

$$d_{mn} = \begin{pmatrix} 0 & 0 & 0 & 0 & d_{15} & 0 \\ 0 & 0 & 0 & d_{24} & 0 & 0 \\ d_{31} & d_{32} & d_{33} & 0 & 0 & 0 \end{pmatrix}. \quad (1)$$

The electrical flux density D of a PVDF sensor is defined as

$$D = \frac{Q}{A} = d_{3n}X_n, \quad (2)$$

where Q is the charge developed by the sensor, A is the conductive electrode area, d_{3n} is the piezoelectric coefficient for the axis of applied stress and X_n is the stress applied in the relevant direction [7]. For the electrical axis m is always 3 since the electrodes are on the top and at the bottom of the film. For the mechanical axis n can be 1, 2 or 3 since the stress can be applied to any of these axes [7].

The PVDF material is also pyroelectric: as the film is heated the dipoles within the film exhibit random motion by thermal agitation, causing a reduction in the average polarization and thus generating a charge [7]. Also, the piezoelectric coefficients of the PVDF material tend to increase with temperature [7]. The temperature dependence of piezoelectric coefficient d is reported e.g. in references [7], [21] and [23].

Table I lists the typical properties of a commercial 28 µm thick PVDF material. The unmetallized film used in this study

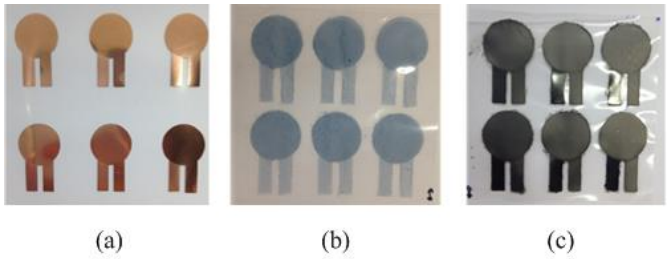

Fig. 1. The sensors with a) copper electrodes (reference) and solution-processable electrode materials (Phene-ink (b) and Vor-ink (c)).

was manufactured by Measurement Specialties Inc. (Hampton, VA, USA).

B. Inks

Two commercially available graphene-based printable inks were used in this work. The first graphene ink PHENE+ I3015 (referred as Phene-ink later) formulated for ink-jet printing was purchased from Innophene Co. (Bangkok, Thailand). The ink has a solid content of 0.6 % of weight. The ink contains 1-5 % of weight polymer and 1–5 % of weight graphene as well as small amounts of organic solvents such as diethylene glycol and ethanol. Since the ink is made for ink-jet printing, it has low solid content and low viscosity. Low graphene content makes Phene-ink film quite transparent.

The second graphene ink Vor-ink X103 (referred as Vor-ink later) formulated for screen printing was purchased from Vorbeck Materials Corp. (Jessup, MD, USA). This ink has a solid content of 15-17 % of weight. Vor-ink is highly concentrated and highly viscous as it is made for screen printing.

C. Electrode fabrication

A manual airbrush was used for spray-coating of the ink-jet formulated Phene-ink electrodes whereas a plastic doctor blade was used for blade-coating of the screen formulated Vor-ink electrodes. The selection of suitable deposition methods for each ink was done based on the ink viscosity. Similar electrodes were subsequently patterned on each side of the PVDF substrate and baked separately after each pattern. Phene-ink was baked for 7 min at 60 °C per side plus an additional 7 min at 60 °C to improve the adhesion to the substrate. Vor-ink was baked for 9 min at 60 °C per each side. In the case of Phene-ink the spray coating was done on top of a hot plate (60 °C) which enhances evaporation of solvent decreasing the drop formation and produces better quality electrodes. For both inks, a mechanical mask made of a 125 µm thick polyethylene terephthalate (PET) film was used to produce electrode patterns on a PVDF substrate.

Copper electrodes for the reference sensor were fabricated by e-beam evaporation (Leopold). A 100 nm thick film of copper was subsequently evaporated on both sides of the PVDF substrate by using a mechanical mask to produce the sensor electrode pattern. Metal evaporation is a standard deposition method for the fabrication of highly conducting and homogeneous metal films and was thus chosen as a reference method to fabricate electrodes on the PVDF substrate.

The sensors with copper electrodes and solution-processed electrodes are shown in Fig. 1. Fig. 1 shows all the sensors fabricated, however, only four sensors of each type are used in the sensor characteristics testing. A complete row of sensors (marked as R1-1, R1-2 and R1-3) and the first sensor from the second row (marked as R2-1) were chosen for the tests. Fig. 2 shows the sensor dimensions in detail. The sensor electrodes have a circular shape with a diameter of 15 mm. The total length of the sensor is 25 mm.

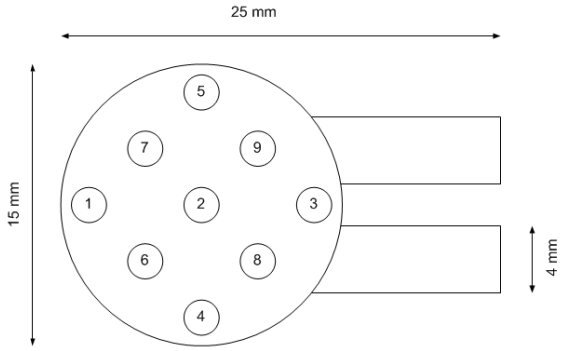

Fig. 2. The sensor dimensions. The excitation positions for the sensor sensitivity measurements are also marked in the figure.

D. Electrode characterization

A multimeter (Keithley 3435 100 W SourceMeter) and an in-house four-point probe were used in sheet resistance measurements [10]. Sheet resistance was measured from five different positions from each fabricated electrode. The four-point probe has four spring probes which are placed in line with equal spacing (s = 3 mm). Finally, the corrected sheet resistance is calculated as

$$R_S = G\frac{\pi}{\ln 2}\frac{V}{I}, \tag{3}$$

where I is the applied current between the two outermost probes, V is the measured voltage between the two innermost probes and G is an additional geometric correction factor, which is determined by sample dimensions and the probe spacing [24]. The geometric factor used for the round shape electrode patterns was G = 0.7419.

E. Adhesion test method

The adhesion of the deposited electrodes on the PVDF material was measured using the tape test method. Adhesion classification is done according to the ASTM standard D 3359-97 (Standard Test Methods for Measuring Adhesion by Tape Test) by applying and removing pressure sensitive tape over cuts made in the ink [25]. In the Test Method B, classification 5B refers to the case where adhesion is very good and no material is detached from the electrode layer. Classification 0B refers to the case where over 65 % of the material has detached from the electrode layer.

F. Testing of sensor characteristics

The Brüel & Kjaer Mini-Shaker Type 4810 was used in the sensor testing. The shaker generates a dynamic excitation force with force rating of 10 N sinusoidal peak and has a

frequency range from DC to 18 kHz. A sinusoidal input for the shaker was provided with a Tektronix AFG3101 function generator. A commercial high sensitivity dynamic force sensor (PCB Piezotronics, model number 209C02) was used as a reference sensor for the dynamic excitation force. The sensor was connected to a sensor signal conditioner (PCB Piezotronics, Model 442B06) with a low-noise coaxial cable. A load cell (Measurement Specialties Inc., model number ELFS-T3E-20L) was used as reference sensor to measure the static force between the sample and shaker's piston. A pretension, which is producing static force, is needed to keep the sample in place and to prevent the piston jumping off the surface during the measurement. A static force of approximately 3 N was used in the measurements.

The measurement setup is previously reported by Kärki *et al*. [8]. Similar measurements are also done by e.g. Seminara *et al*. [26]. To measure the sensor characteristics in normal force direction (n = 3), the sensor was placed horizontally on the metal plate. A 125 µm thick PET film was used under and on top of the sensor for electrical insulation. The charge developed by the sensor was measured with a custom-made combination of a charge amplifier and a 16-bit AD-converter. The connection to the AD-converter from the sensor was provided via coaxial wires and crimp connectors (Nicomatic Crimplex). The AD-converter had additional channels for sampling also the voltage signals from the reference sensors. The amplification of each measurement channel of the converter was calibrated prior to the measurements. Fig. 3 illustrates the sensor testing measurement setup.

The sensor operation was evaluated by measuring the sensor sensitivity, nonlinearity, hysteresis and the effects of frequency and temperature, further presented in the following Sections.

1) Sensor sensitivity

The sensor was excited with an approximate force of 1.3 N (peak to peak), measured with the reference dynamic force sensor, and caused by applying a dynamic, sinusoidal 2 Hz input signal of 1000 mV (peak to peak) to the shaker. The excitation was done by applying the force to 9 different positions on the sensor, one at a time (see Fig. 2). The same positions were excited from both sides of the sensor, resulting in a total of 18 excitations per sensor.

The measured data was processed to solve the sensitivity of the sensor to the force. The sensitivity was obtained by dividing the charge generated by the sensor with the force obtained with the dynamic force sensor. The unit of sensitivity is thus pC/N. Since the excitation force was sinusoidal, the sensitivity can be calculated simply by dividing the amplitudes of the respective signals. Possible baseline drift in the signals was removed with high-pass filtering before the sinusoidal amplitudes were solved by fitting sinusoidals to the signals as described in the IEEE Standard for Digitizing Waveform Recorders (IEEE Std 1241) [27].

2) Nonlinearity and hysteresis

The charge developed by the sensor was measured as a function of dynamic excitation force to determine the nonlinearity of the sensor. The amplitude of the dynamic excitation force was altered from approximately 0.1-5 N (input signal 100-4000 mV (peak to peak)) with constant frequency of 2 Hz. Since the shaker's piston was 4 mm in diameter, the dynamic force range corresponds to pressures from 10 kPa to 400 kPa. This pressure range is suitable to be used for example in plantar pressure measurements.

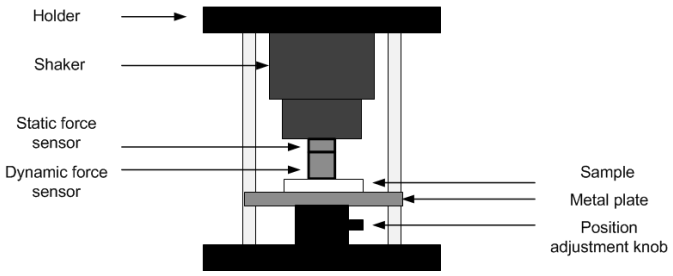

Fig. 3. The sensor testing measurement setup.

The hysteresis error is defined as a deviation of the sensor's output at a specified point of the input signal when it is approached from the opposite directions [28]. Here the hysteresis is determined by measuring the sensor charge as a function of dynamic excitation force, first by increasing the force and then by decreasing the force. The dynamic excitation force range was approximately 0.7-2.5 N (input signal 500-2000 mV (peak to peak)) with constant frequency of 2 Hz.

3) Frequency effects

To evaluate the effect of dynamic excitation force frequency, the frequency was altered from 2 Hz to 100 Hz (2, 5, 10, 20, 40, 60, 80 and 100 Hz) with constant dynamic excitation force (input signal of 1000 mV (peak to peak)). This frequency range is suitable for several sensing applications. In plantar pressure measurement, for example, the frequency content is primarily contained below 10 Hz [29].

4) Temperature effects

To evaluate the effect of temperature, the temperature was altered from +10 °C to +40 °C with constant dynamic excitation force (input signal of 1000 mV (peak to peak)) and frequency (2 Hz). The shaker's operating temperature (+5 to + 40 °C) limits the temperature to this range. The shaker was placed in a temperature test chamber (Vötsch 4021) and the temperature was raised from 10 °C to 40 °C with 10 °C steps. In each temperature the sensitivities of all the twelve sensors were measured, one at a time. The temperature of the test chamber was allowed to stabilize about 30 minutes before starting the measurements in each temperature.

III. Results

A. Sheet resistance

Table II shows the sheet resistance measurement results for each sensor type (reference sensors with copper electrodes and sensors with Phene-ink and Vor-ink electrodes). Four sensors

TABLE II
SHEET RESISTANCE MEASUREMENT RESULTS.

Electrode	Sample name, R_S (Ω/□)			
	R1-1	R1-2	R1-3	R2-1
Cu ref. El-1	1.0 ± 0.2	1.0 ± 0.2	1.0 ± 0.2	1.0 ± 0.2
Cu ref. El-2	1.0 ± 0.2	1.0 ± 0.2	1.0 ± 0.2	1.0 ± 0.2
Phene-ink El-1	116.2 ± 8.8	110.8 ± 4.1	115.1 ± 0.4	130.4 ± 1.6
Phene-ink El-2	88.6 ± 6.8	82.9 ± 5.1	104 ± 16	102.5 ± 2.7
Vor-ink El-1	17.0 ± 0.6	17.4 ± 0.1	14.3 ± 0.1	15.6 ± 0.5
Vor-ink El-2	18.9 ± 1.1	17.4 ± 0.5	17.4 ± 0.5	17.8 ± 0.8

TABLE III
ADHESION TEST RESULTS.

Electrode	Adhesion classification	Interpretation
Cu ref. El-1	5B	0% detached
Cu ref. El-2	5B	0% detached
Phene-ink El-1	3B	5-15% detached
Phene-ink El-2	3B	5-15% detached
Vor-ink El-1	2B	15-35% detached
Vor-ink El-2	2B	15-35% detached

of each type were measured, marked as R1-1, R1-2, R1-3 and R2-1, as discussed earlier in Section IIC. Sheet resistances were measured from all electrodes (electrodes 1 and 2, later El-1 and El-2). The results are presented as mean sheet resistances ± standard deviations.

The copper electrodes showed good conductivity with the average sheet resistance of 1.0 Ω/□, whereas the Vor-ink electrodes showed a lower conductivity with the average sheet resistance of 17.4 Ω/□. The Phene-ink electrodes showed a higher sheet resistance of 105.0 Ω/□, which is due to the thin ink layer which is needed to obtain the transparency of the electrodes.

B. Adhesion tests

The adhesion tests were performed after the sensor characteristics measurements. The results are presented in Table III. The evaporated copper electrodes have a very good adhesion to the PVDF substrate, while the solution-processable electrode materials have the lower adhesion. The adhesion of the Vor-ink electrode layer was found to be the lowest, possibly since the Vor-ink electrode layer was thicker than the copper and Phene-ink electrode layers. In addition to the lower adhesion, it also showed low cohesion forces inside the electrode layer.

C. Sensor sensitivity

Table IV shows the sensitivity measurement results for each sensor type. The results are shown as mean sensitivity ± standard deviation of 18 excitations per sensor. Metallized reference sensors showed the highest sensitivity values of (31.1 ± 1.4) pC/N whereas the Vor-ink sensors showed the lowest sensitivity values of (21.4 ± 1.3 pC/N). The sensors with Phene-ink electrodes had sensitivities of about the average of those ((26.2 ± 2.2) pC/N). The lowest sensitivity values in the case of the Vor-ink sensors are expected to be due to poor adhesion of the material to the PVDF film (see Table III). Also, the thickness of the Vor-ink electrode layer was several micrometers, which is much more than the thickness of the Phene-ink electrode layer. Instead, metallized sensors showed highest sensitivities since those have high adhesion and high electrical conductivity.

TABLE IV
SENSITIVITY MEASUREMENT RESULTS PRESENTED AS MEAN SENSITIVITY ± STANDARD DEVIATION OF 18 EXCITATIONS PER SENSOR.

Electrode	Sample name, Sensitivity (pC/N)			
	R1-1	R1-2	R1-3	R2-1
Cu ref.	31.3 ± 1.3	30.9 ± 1.3	31.1 ± 0.8	31.1 ± 2.0
Phene-ink	26.5 ± 1.6	26.5 ± 2.4	26.8 ± 2.4	25.1 ± 2.0
Vor-ink	20.7 ± 1.3	21.5 ± 0.9	21.6 ± 1.5	21.7 ± 1.3

D. Nonlinearity and hysteresis

Fig. 4 shows the charge developed by the sensor as a function of dynamic excitation force. Fig a. presents the values measured with reference sensor and b. and c. the values measured with Phene-ink and Vor-ink sensors.

Fraden defines the nonlinearity as a maximum deviation of a real transfer function from the approximation straight line [28]. Here the nonlinearity is determined by fitting a first degree polynomial to data in a least-squares sense (Matlab function polyfit). Fig. 4d shows an example of the fitting (reference sensor R1-1: $y = 39.07x - 11.26$). In Figs. 4a-c the sensor R1-1 is shown with circles, sensor R1-2 with crosses, sensor R1-3 with squares and sensor R2-1 with diamonds. The fitted polynomial in Fig. 4d is shown with a dashed line. Instead of showing the maximum deviation from the approximation straight line, the nonlinearity is presented here as the mean ± standard deviation of data point deviations from the fitted polynomial, that is, the change in sensor charge, marked as ΔQ. The results for each sensor are shown in Table V. The unit of deviation is pC. As shown in Fig. 4, the PVDF sensors with both reference copper and graphene-based electrodes are rather linear.

Fig. 5 shows the hysteresis measurement results. The measurements made by increasing the dynamic excitation force are marked with circles and the measurements made by decreasing the force with crosses. Sensors R1-1 are drawn with blue solid line, sensors R1-2 with red dashed line, sensors R1-3 with green dotted line and sensors R2-1 with black dash-dot line. Fig. 5d. shows a single example of the hysteresis measurement results (reference sensor R1-1). As can be seen, the hysteresis of the sensors is negligible and thus the numerical values for hysteresis are not determined. For example, for reference sensor R1-1 the maximum difference

TABLE V
NONLINEARITY MEASUREMENT RESULTS PRESENTED AS MEAN ± STANDARD DEVIATION OF DATA POINT DEVIATIONS FROM THE FITTED POLYNOMIAL.

Electrode	Sample name, ΔQ (pC)			
	R1-1	R1-2	R1-3	R2-1
Cu ref.	7.3 ± 5.1	4.1 ± 3.0	6.8 ± 3.1	7.3 ± 4.3
Phene-ink	6.8 ± 4.2	4.7 ± 3.9	6.4 ± 3.5	3.3 ± 2.0
Vor-ink	4.1 ± 2.4	4.4 ± 2.7	5.2 ± 2.4	3.9 ± 2.8

TABLE VI
CHANGE IN SENSOR SENSITIVITY DUE TO CHANGING DYNAMIC EXCITATION FORCE FREQUENCY (FROM 2 HZ TO 100 HZ).

Electrode	Sample name, ΔS (pC/N)			
	R1-1	R1-2	R1-3	R2-1
Cu ref.	0.5 ± 0.3	1.0 ± 0.5	0.8 ± 0.5	0.5 ± 0.3
Phene-ink	0.6 ± 0.3	1.2 ± 1.1	0.8 ± 0.8	1.6 ± 1.1
Vor-ink	0.3 ± 0.3	0.3 ± 0.2	0.7 ± 0.3	0.6 ± 0.5

TABLE VII
CHANGE IN SENSOR SENSITIVITY DUE TO CHANGING AMBIENT TEMPERATURE (FROM +10 °C TO +40 °C)

Electrode	Sample name, ΔS (pC/N)			
	R1-1	R1-2	R1-3	R2-1
Cu ref.	2.7 ± 0.5	2.0 ± 0.8	1.9 ± 0.7	2.0 ± 1.5
Phene-ink	1.9 ± 1.4	1.8 ± 1.5	1.4 ± 1.0	2.13 ± 1.41
Vor-ink	1.5 ± 1.3	1.4 ± 0.8	1.5 ± 0.6	1.8 ± 1.4

between increasing and decreasing measurements was 0.96 pC and for the Phene-ink and Vor-ink R1-1 sensors 1.20 pC and 0.34 pC, respectively.

E. Frequency effects

Fig. 6 shows the sensor sensitivity as a function of dynamic excitation force frequency. Similar markings are used as in Fig. 4. With an ideal sensor, the sensitivity would be a constant and thus independent on the excitation force frequency. Hence the effect of frequency is determined here by fitting a zeroth degree polynomial to data in a least-squares sense (reference sensor R1-1: $y = 29.24$).

The effect of frequency is presented here as the mean ± standard deviation of data point deviations from the fitted polynomial, that is, the change in sensor sensitivity, marked as ΔS. The changes in sensor sensitivities due to the changing excitation force frequency for each sensor type are shown in Table VI. The unit of deviation is pC/N.

As seen from Fig. 6, the sensitivity is almost a constant and independent on the excitation force frequency. However, besides the random fluctuation of the sensitivity, also a weak downward linear trend is seen with some sensors. Typically the linear trend of the signal is removed before the computation of the statistical variables. However, here the linear trend of the signal is an unwanted property and thus it is included in the computation.

F. Temperature effects

Fig. 7 shows the sensor sensitivity as a function of temperature. Again, similar markings are used as in Fig. 4. As with frequency measurements, the sensitivity should be independent on the temperature and thus, the approximation straight line is determined by fitting a zeroth degree polynomial to data in a least-squares sense (reference sensor R1-1: $y = 30.18$). The changes in sensor sensitivities due to the changing ambient temperature for each sensor type are shown in Table VII. Similar marking are used as in Table VI.

Temperature variations affect the PVDF sensor in two ways, due to the pyroelectric effect and due to the temperature dependence of the piezoelectric d_{33} coefficient, as already discussed in Section IIA. The error caused by the pyroelectric effect is seen only at low frequencies [7] and provides slow changes in signals. When the PVDF material has reached a stabilizing temperature, the material properties remain constant with time [7] and thus the pyroelectric effect is not a remarkable problem. Instead, the piezoelectric coefficients of the PVDF material tend to increase with temperature [7] and this was seen also here as the increase in sensitivity values as a function of ambient temperature. If the PVDF sensors are used

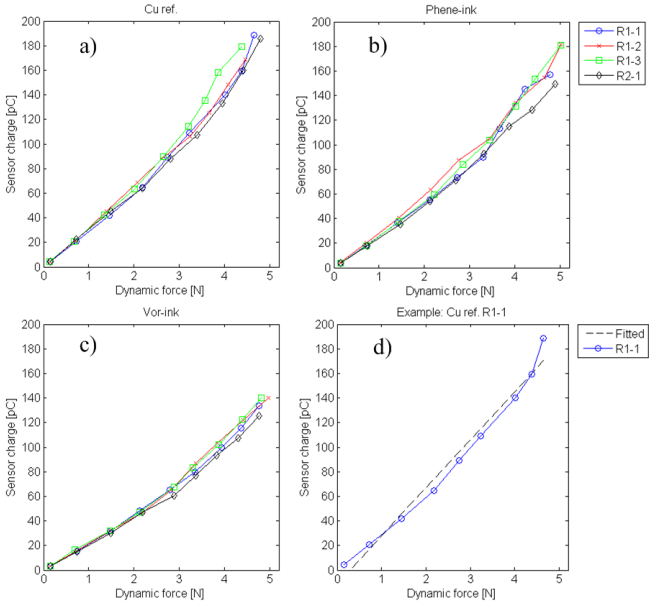

Fig. 4. The linearity measurement results for a) reference, b) Phene-ink and c) Vor-ink sensors. Figure d) shows a more detailed example of linearity measurement results (reference sensor R1-1, $y = 39.07x$-11.26).

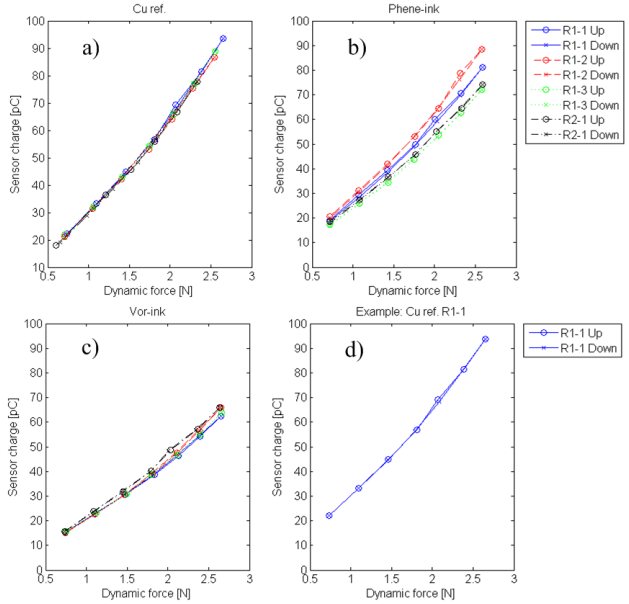

Fig. 5. The hysteresis measurement results for a) reference, b) Phene-ink and c) Vor-ink sensors. Figure d) shows a more detailed example of hysteresis measurement results (reference sensor R1-1).

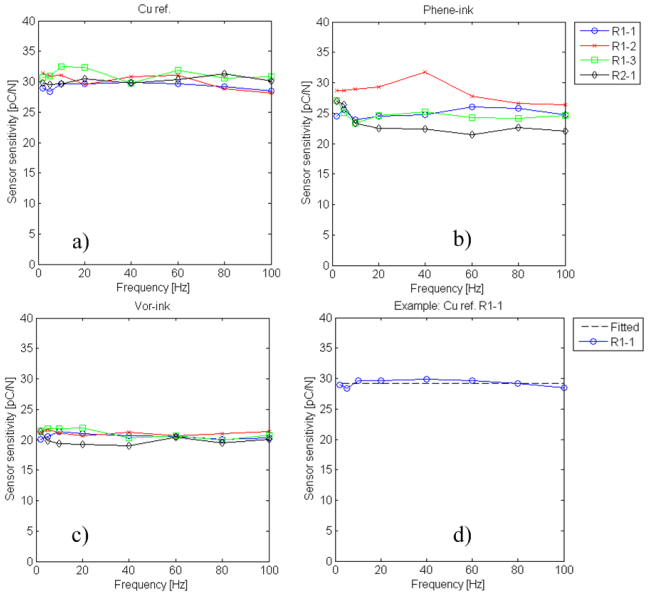

Fig. 6. The frequency measurement results for a) reference, b) Phene-ink and c) Vor-ink sensors. Figure d) shows a more detailed example of frequency measurement results (reference sensor R1-1, y = 29.24).

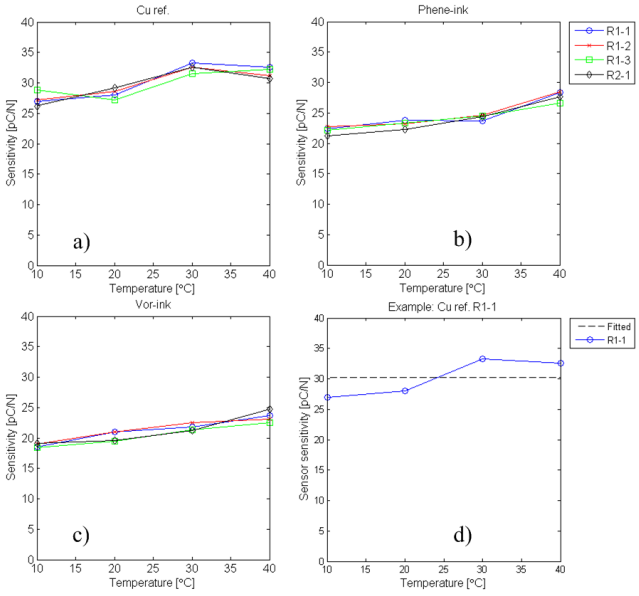

Fig. 7. The temperature measurement results for a) reference, b) Phene-ink and c) Vor-ink sensors. Figure d) shows a more detailed example of temperature measurement results (reference sensor R1-1, y = 30.18).

in conditions where the temperature is higher than the room temperature, for example in in-shoe plantar pressure measurements, the sensitivity values measured in these temperatures should be used instead when computing the pressure values. However, the sensitivity values in different temperatures presented in this study are preliminary results and more complete temperature measurements are still needed to fully understand the operation in temperatures above room temperature.

IV. Discussion and Conclusions

Here, the piezoelectric PVDF sensors were fabricated using graphene-based solution-processable electrode materials. The sensor characteristics (sensitivity, nonlinearity, hysteresis and the effects of frequency and temperature) were measured and compared with the characteristics of reference sensor (copper electrodes). The sensors with graphene-based electrodes were found to be functional and the sensor characteristics were similar to those of the reference sensors. Also, each set of four sensors made of the same electrode material showed very similar results in the sensor characteristics measurements.

The measured sensitivities of the sensors with graphene-based electrodes were slightly lower than in the case of the metallic electrodes. This is most likely related to the lower conductivity of the graphene-based electrodes. As shown in the results, there is more variation between the samples in the case of the Phene-ink sensors when compared with the Vor-ink or copper reference sensors. The same occurrence can also be seen in the results of other sensor property tests (see e.g. Fig. 5b and 6b). This is most likely related to higher sheet resistance of the Phene-ink electrodes as well as the larger variation in sheet resistances between the Phene-ink samples (see Table II).

The novel sensors with graphene-based electrodes are linear, hysteresis error is negligible, and operation under changing frequency (up to 100 Hz) is rather stable. The change in ambient temperature somewhat affects the sensor sensitivities as also reported in references [7], [21] and [23]. However, more measurements in this area are still needed. The sensors presented in this study are designed especially for plantar pressure measurements and they seem to be a promising sensor type for measurements of this kind. The same sensors, however, can also be used in several other sensing applications.

The lack of need for high temperature treatment makes nanostructural carbon based materials favorable for temperature sensitive PVDF substrate. Also, use of the solution-processable materials enables low-cost and high throughput mass manufacturing of the PVDF sensors in a desired customized shape and size. Both materials, however, have their pros and cons. The Phene-ink sensors, for instance, have more variation in the values measured with the sensor. However, the sensors have higher sensitivity than the Vor-ink sensors have, and also, potentially transparent sensors are possible to make by using the Phene-ink electrode material. The Vor-ink sensors, instead, provide more stable results than the Phene-ink sensors but the ink was easily peeled off from the substrate (see Table III). Thus, in the case of the Vor-ink electrode material, there is a need for an adhesion promoter layer or pre-treatment prior to the electrode deposition in future.

Acknowledgment

The authors acknowledge funding from the Academy of Finland (Dec. No. 137669 and 138146).

REFERENCES

[1] P. Avouris, Z. Chen and V. Perebeinos, "Carbon-based electronics", Nature Nanotechnology, vol. 2, pp. 605–15, 2007.

[2] F. Bonaccorso, Z. Sun, T. Hasan and A.C. Ferrari, "Graphene photonics and optoelectronics", Nature Photonics, vol. 4, pp. 611–622, 2010.

[3] K. S. Novoselov, V. I. Fal′ko, L. Colombo, P. R. Gellert, M. G. Schwab and K. Kim, "A roadmap for graphene", Nature, vol. 490, pp. 192–200, 2012.

[4] S. Tuukkanen, M. Hoikkanen, M. Poikelispää, M. Honkanen, T. Vuorinen, M. Kakkonen, J. Vuorinen and D. Lupo, "Stretching of Solution Processed Carbon Nanotube and Graphene Nanocomposite Films on Rubber Substrates", Synthetic Met, vol. 191, pp. 28-35, 2014.

[5] T. Vuorinen, M. Zakrzewski, S. Rajala, D. Lupo, K. Palovuori, J. Vanhala and S. Tuukkanen, "Printable, transparent and flexible touch panels working in sunlight and moist environments", Adv Functional Mater, in press.

[6] S. Lehtimäki, M. Li, J. Salomaa, J. Pörhönen, A. Kalanti, S. Tuukkanen, P. Heljo, K. Halonen and D. Lupo, "Performance of printable supercapacitors in an RF energy harvesting circuit", Int J Elec Power, vol. 58, pp. 42–46, 2014.

[7] Measurement Specialties Inc., "Piezo film sensors, Technical manual". Available online at: http://www.meas-spec.com (accessed 5 May 2014).

[8] S. Kärki, J. Lekkala, H. Kuokkanen and J. Halttunen, "Development of a piezoelectric polymer film sensor for plantar normal and shear stress measurements", Sensors Actuat A-Phys, vol. 154, pp. 57-64, 2009.

[9] P.R. Cavanagh, F.G. Hewitt, J.E. Perry. "In-shoe plantar pressure measurements: a review", The Foot, vol. 2, pp. 185-194, 1992.

[10] S. Tuukkanen, T. Julin, V. Rantanen, M. Zakrzewski, P. Moilanen, K. E. Lilja and S. Rajala, "Solution-processible electrode materials for a heat-sensitive piezoelectric thin-film sensor", Synthetic Met, vol. 162, pp. 1987-1995, 2012.

[11] S. Tuukkanen, T. Julin, V. Rantanen, M. Zakrzewski, P. Moilanen and D. Lupo, "Low-Temperature Solution Processable Electrodes for Piezoelectric Sensors Applications", Jpn J Appl Phys, vol 52, 05DA06, 2013.

[12] S. Kärki, M. Kiiski, M. Mäntysalo and J. Lekkala, "A PVDF sensor with printed electrodes for normal and shear stress measurements on sole", in Proc. IMEKO XIX World Congress, Lisbon, Portugal, 2009, pp. 1765-1769.

[13] L. Seminara, L. Pinna, M. Valle, L. Basiricò, A. Loi, P. Cosseddu, A. Bonfiglio, A. Ascia, M. Bisco, A. Ansaldo, D. Ricci and G. Metta. "Piezoelectric polymer transducer arrays for flexible tactile sensors", IEEE Sensors Journal, vol. 13, pp. 4022-4029, 2013.

[14] C.S. Lee, J.Y. Kim, D.E. Lee, J. Joo, B.G. Wagh, S. Han, Y.W. Beag and S.K. Koh, "Flexible and transparent organic film speaker by using highly conducting PEDOT/PSS as electrode", *Synthetic Met*, vol. 139, pp. 457–461, 2003.

[15] V. H. Schmidt, L. Lediaev, J. Polasik and J. Hallenberg, "Piezoelectric Actuators Employing PVDF Coated with Flexible PEDOT-PSS Polymer Electrodes", *IEEE T Dielect El In*, vol 13, pp. 1140-1148, 2006.

[16] M. Zirkl, A. Sawatdee, U. Helbig, M. Krause, G. Scheipl, E. Kraker, P. A. Ersman, D. Nilsson, D. Platt, P. Bodö, S. Bauer, G. Domann and B. Stadlober, "An All-Printed Ferroelectric Active Matrix Sensor Network Based on Only Five Functional Materials Forming a Touchless Control Interface", *Adv Mater*, vol. 23, pp. 2069–2074, 2011.

[17] C. Rendl, P. Greindl, M. Haller, M. Zirkl, B. Stadlober and P. Hartmann, "PyzoFlex: Printed Piezoelectric Pressure Sensing Foil", in *Proc. 25th Symposium on User Interface Software and Technology*, Cambridge, USA, 2012, pp. 509-518.

[18] G. Eberle, H. Schmidt and W. Eisenmenger, "Piezoelectric polymer electrets", IEEE T Dielect El In, vol. 3, pp. 624-646, 1996.

[19] J.S. Harrison and Z. Ounaies, "Polymers, Piezoelectric", in Encyclopedia of Smart Materials, John Wiley & Sons, 2002.

[20] J. F. Nye, Physical properties of crystals. Oxford University Press, London, 1969.

[21] Q.M. Zhang, V. Bharti and G. Kavarnos, "Poly(Vinylidene Fluoride) (PVDF) and its Copolymers", in Encyclopedia of Smart Materials, John Wiley & Sons, 2002.

[22] T. Furukawa, "Piezoelectricity and pyroelectricity in polymers", IEEE T Electr Insul, vol. 24, pp. 375-394, 1989.

[23] A. Vinogradov, "Piezoelectricity in Polymers", in Encyclopedia of Smart Materials, John Wiley & Sons, 2002.

[24] H. Topsoe, "Geometric correction factors in four- point resistivity measurement", Bulletin no. 472-13, 1968. Available online at: http://www.fourpointprobes.com/haldor.html (accessed 5 May 2014).

[25] Standard Test Methods for Measuring Adhesion by Tape Test, United States ASTM D3359-97, 1997.

[26] L. Seminara, M. Capurro, P. Cirillo, G. Cannata and M. Valle. "Electromechanical characterization of piezoelectric PVDF polymer films for tactile sensors in robotics applications", Sens. Actuators A: Phys., vol 169, pp. 49-58, 2011.

[27] IEEE Standards Board (1994), IEEE Standard for Digitizing Waveform Recorders (IEEE Std 1057-1994), doi: 10.1109/IEEESTD.1994.122649.

[28] J. Fraden, Handbook of modern sensors: Physics, designs, and application. 4th edition, Springer, New York, 2010.

[29] G.F. Harris, K.R. Acharya and R.A. Bachschmidt, "Investigation of spectral content from discrete plantar areas during adult gait: an expansion of rehabilitation technology", IEEE T Rehab Eng, vol. 4, pp. 360-374, 1996.

Satu Rajala (née Kärki) received her M.Sc. and D.Sc. (Tech.) degrees from Tampere University of Technology (TUT), Finland in 2004 and 2009, respectively. She has been working in the Department of Automation Science and Engineering, TUT since 2003. Her interest areas include sensors, sensor materials and sensor systems for physiological measurements.

Sampo Tuukkanen received Ph.D. in physics/nanoelectronics from University of Jyväskylä, Finland in 2006. He had two-year postdoc (2007-2009) in the Molecular Electronics Group in CEA/Saclay, France, working on carbon nanotubes. Since 2009 he's been working as a senior researcher at Laboratory for Future Electronics at the Tampere University of Technology, Department of Electronics and Communications Engineering. His interest areas are printed electronics, sensors and energy harvesting and storage systems.

Jouko Halttunen received his M.Sc. degree in electrical engineering from University of Oulu, Finland in 1975 and D.Sc. (Tech) degree in electrical engineering from Tampere University of Technology (TUT), Finland, in 1992. Since 1995 he has been associate professor and professor of measurement technology at the Department of Automation Science and Engineering, TUT. His interest areas are metrology, sensors and measurement systems.